Isothermal Crystallization of Hydrogenated Sunflower Oil: I—Nucleation

M.L. Herrera[a,*], C. Falabella[b], M. Melgarejo[b], and M.C. Añón[a]

[a]Centro de Investigación y Desarrollo en Criotecnología de Alimentos (CIDCA) (UNLP - CONICET), La Plata 1900, Provincia de Buenos Aires, Argentina, and [b]Molinos Río de La Plata S.A., Buenos Aires 1323, Argentina

ABSTRACT: Nucleation kinetics of sunflower seed oil, which was hydrogenated under two different conditions, was studied by means of a polarized light microscope and an optical setup with a laser as the light source. When the laser was used, observed induction times were shorter than the ones measured by the microscope. The laser method was found to be more sensitive and accurate. Two different crystallization behaviors were found depending on the chemical composition of the samples. Samples with high content of trielaidin crystallized in the β form at temperatures close to the melting points. They exhibited both β′ and β forms depending on crystallization temperature, as happens in natural semisolid fats such as palm oil. Samples with high content of mixed oleic and elaidic triacylglycerols crystallized in the β′ form even at temperatures close to the melting points and they did not show β form under the conditions used in this study. Activation free energies of nucleation for hydrogenated sunflower seed oil were low for the two hydrogenation conditions. It can be concluded that nucleation of sunflower seed oil is a fast process and initially needs low supercooling. These results are also important from a practical point of view for processing design, especially in regards to processes in which fats should be completely crystallized by the end of the production line.

JAOCS 75, 1273–1280 (1998).

KEY WORDS: Hydrogenation, isothermal crystallization, kinetics, laser, microscopy, nucleation, sunflower seed oil.

Hydrogenation and interesterification are among the tools the industry uses to give fats and oils a desired functionality for specific products. Currently, formulators can raise the melting point and solid fat content of fats by (i) hydrogenating oils to different degrees of hardness or (ii) interesterifying a liquid oil with a more saturated oil (1). The aim of the hydrogenation process is the total or partial saturation of the double bonds of unsaturated fats to obtain hard or plastic fats or to improve the stability to oxidation of an oil. The obtained product depends on the nature of the starting oil, the type and concentration of the catalyst used, the concentration of hydrogen, and the experimental conditions under which the reaction takes place (2). Nickel catalyst was reported to catalyze undesirable side reactions such as *cis,trans* isomerization and positional isomerization of double bonds (3). The position of the double bonds affects the melting point of the fatty acid to a limited extent. The presence of different geometric isomers of fatty acids influences the physical characteristics of the fat to a greater extent (4).

Rates of crystal formation, growth, and polymorphic transformation are important to determine processing and storage conditions of oils and fats (5). In food applications, fat crystals with a platelet-like shape must be below 30 μm to avoid a "sandy" mouthfeel. A challenging problem is to control crystallization so that a minimum of solid content can give a homogeneous plastic fat to be used to formulate bread, biscuits, and other products (6). Crystallization kinetics of cocoa butter (7–12), palm oil (13–15), and butterfat (16) have been studied to improve their processing and storage conditions.

Crystallization can generally be classified in two steps: nucleation and growth. Nucleation involves the formation of molecular aggregates which exceeded a critical size and therefore are stable. Once nuclei have formed, they grow and develop into crystals. The nucleation process depends on supersaturation or supercooling (16).

The aim of this study is to investigate the nucleation behavior of sunflower seed oil which was hydrogenated under two different conditions (selective and nonselective). Two methods were used to measure induction times of crystallization and were compared.

MATERIALS AND METHODS

Starting oils. Hydrogenation was performed in the commercial hydrogenation plant of Molinos Río de La Plata S.A. (Buenos Aires, Argentina). A batch slurry reactor and a supported nickel catalyst at a concentration of 0.05% were used. Two different hydrogenation conditions were selected: (i) high temperature of reaction and low pressure of hydrogen gas (463 K, 1 kg/cm^2), and (ii) low temperature and high pressure (443 K, 2.5 kg/cm^2). There is a general agreement that high reaction temperatures promote formation of *trans* isomers. High concentration of hydrogen gas results in low selectivity and low isomer content, while low concentration of hydrogen gas results in high selectivity and high *trans* isomer content. By using these two temperature and pressure condi-

*To whom correspondence should be addressed at CIDCA, Casilla de Correo 553, (1900) La Plata, Provincia de Buenos Aires, Argentina.
E-mail: mcanon@isis.unlp.edu.ar

tions, we intended to obtain two oils with different chemical compositions and to investigate whether or not they had different crystallization behaviors. Samples were collected every 15 min, beginning 45 min after the start of the reaction. Reactions were stopped after 145 and 150 min, respectively. Samples collected at the same time in both processes had close iodine values and had a solid fat content such that they could be used as plastic fats in different industrial applications, such as the formulation of margarine or shortenings. Dropping points of the samples were determined using a Mettler FP 80 dropping point apparatus (Mettler Instruments A.G., Greifensee-Zurich, Switzerland), using a heating rate of 1°C/min. The starting sunflower seed oil had an iodine value of 134. Iodine values and Mettler dropping points (MDP) of all collected samples are reported in Table 1.

Gas–liquid chromatography (GLC). Fatty acid methyl esters (FAME) were prepared by transesterification with a mixture of methanol/benzene (3:1) and 3% wt/vol sulfuric acid. They were analyzed in a 5890 A chromatograph (Hewlett-Packard, Palo Alto, CA) with a fused-silica capillary column, 0.25 µm film, Optima 240-DF-0.25 of 60 m length and 0.25 mm i.d. (Macherey-Nagel, Düren, Germany). Hydrogen was used as the carrier gas and column head pressure was 140 KPa. Temperature conditions were as follows: start 423 K, rate 1.8 K/min, final 483 K. Standards were purchased from Sigma Chemical Co. (Sigma, St. Louis, MO).

Silver–high-performance liquid chromatography (Ag–HPLC). Triacylglycerols (TAG) were analyzed in a Waters HPLC system consisting of a Waters 600 solvent delivery system with a Waters 717 plus autosampler injector (Waters, Milford, MA) and an evaporative laser light-scattering MK III detector (Varex, Rockville, MD). Nitrogen was used as the nebulizing gas. The solvent system was dichloromethane, dichloroethane, acetone, and acetonitrile (HPLC grade, Merck, Darmstadt, Germany). They were used under multilinear gradient conditions at a solvent flow rate of 0.8 mL/min (Table 2). TAG (200 µg) were injected in dichloromethane. A silver ion-loaded Nucleosil 5 SA column (Macherey-Nagel) of 250 mm length and 4.6 mm i.d. was used. Prior to sample loading, the column was flushed with acetonitrile, methanol, and water (HPLC grade) for 20 min each at 1 mL/min flow rate. An aqueous silver nitrate solution (800 µL; 0.1 g in 1 mL) was injected in 50-µL aliquots. Excess silver nitrate was eluted from the column, and was detected by precipitation with sodium chloride solution. The column was flushed with water, then methanol, and finally acetonitrile, as above in reverse order followed by two blank solvent gradients before use. By using sulfonic acid as a strong cation exchange ligand, and with Ag as a counter ion, a good separation of the *trans* and *cis* isomers can be obtained (17).

TABLE 1
Iodine Values of All Samples Taken During the Two Hydrogenation Processes

First hydrogenation				Second hydrogenation			
Sample	Time (min)	Iodine value	MDP[a] (K)	Sample	Time (min)	Iodine value	MDP (K)
1	45	102	292.4	9	45	98	293.1
2	60	96	295.1	10	60	94	295.7
3	75	86	296.3	11	75	86	296.7
4	90	83	298.0	12	90	78	299.3
5	105	77	300.4	13	105	74	301.3
6	120	70	303.0	14	120	68	305.4
7	135	69	305.2	15	135	67	309.8
8	145	62	306.8	16	150	64	313.4

[a]MDP, Mettler dropping point.

TABLE 2
Multilinear Solvent Gradient Used with Nucleosil 5 SA Column[a]

Time (min)	Dichloromethane/ dichloroethane, 50:50 (%)	Acetone (%)	Acetone/ acetonitrile, 90:10 (%)
0	100	0	0
1	100	0	0
16	50	50	0
41	0	50	50
46	0	50	50
55	100	0	0
75	100	0	0

[a]Macherey-Nagel, Düren, Germany.

Optical microscope. A Leitz microscope model Ortholux II (Ernest Leitz Co., Wetzlas, Germany) with a controlled temperature platform was used to determine temperature and crystal formation times. The temperature was controlled through a programmable Lauda UK 30 cryostat. Ethylene glycol in water (3:1, vol/vol) was used as coolant. The sample was held for 10 min at 353 K, pipetted onto a slide at crystallization temperature, and covered by a slide cover. Selected crystallization temperatures are reported in Table 6. The formed crystals were observed by using polarized light. Magnification of 400× was used for all temperatures. Results are the mean of seven runs and were checked by three different operators.

Laser-polarized light turbidimetry. The crystallization process was also monitored by using an optical setup as described previously (18). A helium–neon laser was used as the light source. A polarizer was between the laser and the cell in which the sample was contained. The light transmitted by the crystals then passed through the second analyzer placed at the cross-Nicols position to the first analyzer. This enabled the photodiode to detect the occurrence of fat crystals. The photosensor output was recorded along with the cell temperature. A typical chart-recorder output of the CdS photodiode, as well as the thermocouple's record for the crystallization of hydrogenated sunflower seed oil, was reported (18). The induction time is defined as the interval between the moment crystallization temperature is reached and the start of crystallization (first deviation from the laser baseline signal). Samples were melted and held at 353 K for 10 min. Then they were crystallized by reducing the temperature to the crystallization temperatures reported in Table 6 at a cooling rate of 5°C/min. Samples 6–8 and 14–16 were also crystallized to all temperatures reported in Figures 2 and 3. The results shown in Table 6 are the average of seven runs. Induction times ob-

tained by the two methods were compared using the paired Student's *t*-test at $P < 0.01$ and $P < 0.05$.

X-ray diffraction (XRD). When the laser signal reached a peak, crystals were filtered through a 53 GA Pyrex filter (pore diameter 5 µm; Aldrich Chemical Company, Milwaukee, WI) under vacuum. Samples included in Figures 2 and 3 were analyzed for their polymorphic form by using a Philips 1730 instrument fitted with a system for temperature control (Philips Argentina S.A., Capital Federal, Argentina). The temperature of the sample holder placed within the refraction chamber was controlled through a programmable Lauda UK 30 cryostat. Ethylene glycol in water (3:1, vol/vol) was used as coolant. $K_{\alpha 1 \alpha 2}$ radiation from copper was used at 40 kV , 20 mA, and a scanning velocity of 2°/min from 1 to 30°.

Calculation of activation free energy of nucleation. The activation free energy of nucleation, ΔG_c, can be evaluated using the Fisher-Turnbull equation:

$$J = (NkT/h) \exp\left(-\Delta G_d/kT\right) \exp\left(-\Delta G_c/kT\right) \quad [1]$$

where J is the rate of nucleation; ΔG_d , activation free energy of diffusion; k, gas constant per molecule; T, temperature; N, number of molecules per cm^3 in liquid phase; and h, Planck's constant. J can be determined experimentally by measuring the induction time (ι) of nucleation which is inversely proportional to J. For a spherical nucleus, the activation free energy of nucleation is related to the surface free energy of the crystal/melt interface, σ, and the supercooling (melting point–crystallization temperature) $\Delta T = (T_m - T_c)$ by $\Delta G_c = (16/3)\ \pi\ \sigma^3\ T_m{}^2/(\Delta H)^2\ (\Delta T)^2$. From plots of log ιT vs. $1/T(\Delta T)^2$ a slope (s) can be evaluated, which allows calculation of the activation free energy of nucleation by $\Delta G_c = sk/(T_m - T_c)^2$. The Fisher-Turnbull equation was originally derived for a single-component system and was proved to be applicable to palm oil, which is a multicomponent system (13). Calculations were made by using the Systat statistical software package (Systat, Inc., Evanston, IL).

RESULTS AND DISCUSSION

GLC. Table 3 shows the fatty acid composition of the starting sunflower seed oil and of all samples collected during both hydrogenation processes. As can be observed from Table 3, the percentage of L ($C_{18:2}$, linoleic acid) was greater in the starting oil and decreased with the time of hydrogenation. $C_{18:2}$ *cis*,*trans* and *trans*,*trans* isomers [linoelaidic acid (Ln) reported all together] increased at the begining of hydrogenation and then remained constant. Stearic acid (S) and elaidic acid (E) ($C_{18:1}$ *trans* isomers all together) always increased, but values of S were slightly higher for the second hydrogenation while the values of E were slightly higher for the first hydrogenation. Oleic acid (O) ($C_{18:1}$ *cis* isomers all together) increased at the begining, were higher for intermediate hydrogenation times (90 to 120 min), then decreased, showing a different behavior than L.

No significant differences were observed in the *trans* fatty acid content between the two hydrogenation procceses, which is surprising. It was expected to obtain a higher *trans* isomer content when selective hydrogenation conditions were used. To obtain further information about the chemical composition of the samples, we analyzed for their TAG composition by Ag-HPLC.

Ag-HPLC. Figure 1 shows the chromatogram corresponding to sample 1. It was taken as an example to show the resolution of the selected HPLC method.

When the starting oil was analyzed, 40 peaks were found. Six of them were the main TAG, and they were identified as OOO, PLO, OLO, PLL, LLO, and LLL (P = palmitic acid) with percentages of 9.9, 10.1, 7.5, 11.7, 23.5 and 29.1, respec-

TABLE 3
Fatty Acid Composition of Original Sunflower Seed Oil and of All Samples Collected During Both Hydrogenation Processes

Sample	$C_{14:0}$	$C_{16:0}$	$C_{18:0}$	$C_{18:1t}$[a]	$C_{18:1c}$[a]	$C_{18:2t}$[b]	$C_{18:2c}$[a]	$C_{20:0}$	$C_{22:0}$
Original	0.1	6.7	3.6	0.7	21.9	—	66.3	0.2	0.5
1	0.1	6.7	7.7	1.8	37.8	8.4	36.7	0.3	0.4
2	0.1	6.8	8.7	2.3	41.7	9.9	29.8	0.2	0.4
3	0.1	6.7	11.0	2.8	46.7	12.1	19.8	0.2	0.5
4	0.1	6.7	13.8	3.9	51.2	12.5	11.0	0.2	0.5
5	0.1	6.8	15.4	4.8	53.2	11.8	6.8	0.3	0.5
6	0.1	6.6	20.7	5.6	50.6	11.7	3.9	0.2	0.5
7	0.1	6.6	24.5	8.9	45.4	12.6	3.0	0.3	0.3
8	0.1	6.7	29.5	9.2	38.8	12.6	2.2	0.3	0.4
9	0.1	6.6	7.5	2.0	42.3	9.1	31.8	0.2	0.4
10	0.1	6.6	10.6	2.3	45.9	10.3	23.7	0.2	0.3
11	0.1	6.6	11.7	2.6	49.4	10.8	18.1	0.2	0.5
12	0.1	6.7	15.6	2.9	52.5	10.9	10.8	0.2	0.3
13	0.1	6.7	16.1	3.5	55.0	12.2	5.7	0.2	0.5
14	0.1	6.7	21.5	4.5	52.6	12.6	1.4	0.2	0.4
15	0.1	6.6	27.6	5.8	46.3	12.2	0.7	0.2	0.4
16	0.1	6.6	31.2	7.6	41.0	12.4	0.4	0.2	0.5

[a]All positional isomers together.
[b]*cis,trans, trans,cis,* and *trans,trans* isomers together.

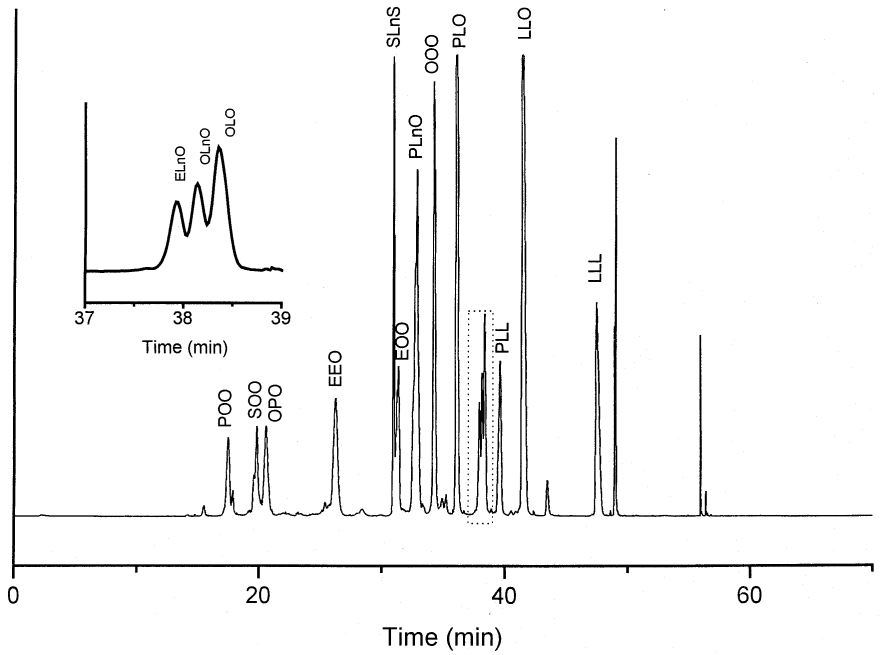

FIG. 1. Silver–high-performance liquid chromatogram of sample 1. Nonlinear gradient: 0.8 mL/min of dichloromethane/dichloroethane/acetone/acetonitrile. Varex evaporative light-scattering detector (Varex, Rockville, MD). Abbreviations: S, stearic acid; P, palmitic acid; O, oleic acid; L, linoleic acid; Ln, linoelaidic acid; E, elaidic acid. A magnification of the area 37–39 min is also shown in the figure.

tively. Their retention times (t_R) are reported in Tables 4 and 5. The others were minor components with percentages less than 1.5.

Tables 4 and 5 show the TAG composition of all samples taken during first hydrogenation process (Table 4) and second hydrogenation process (Table 5). Samples reported in Table 4 correspond to samples 1 to 8 of Table 3 and samples reported in Table 5 correspond to samples 9 to 16 of Table 3.

The percentages of OLO, PLL, LLO, and LLL are greater in the starting oil and, as can be observed from Tables 4 and 5, decreased with the time of hydrogenation until after 105 min they were not found at all. Samples 5–8 (Table 4) and

TABLE 4
Triacylglycerol (TAG) Composition of Samples Taken During the First Hydrogenation

		Sample							
TAG	t_R[a] (min)	1	2	3	4	5	6	7	8
SEE[b]	7.6	—	—	—	—	—	1.1	1.0	2.6
OPE	14.7	—	—	—	—	2.8	2.1	1.8	1.1
OSE	15.5	—	—	—	—	3.9	2.1	2.7	5.2
EEE	17.5	—	—	—	—	2.1	2.9	4.9	4.3
POO	17.9	2.4	2.2	1.7	1.0	1.9	1.4	1.8	2.0
SOO	18.4	2.3	2.5	2.0	1.8	1.0	2.4	1.4	2.2
OPO	20.4	3.4	1.6	1.2	3.6	7.6	18.4	17.3	16.2
EEO	26.2	5.1	11.0	14.2	19.7	29.8	31.9	39.2	40.1
SLnS	30.9	5.6	8.5	10.9	13.3	14.2	10.2	10.2	10.8
EOO	31.2	4.3	7.6	11.3	10.8	8.7	4.6	6.3	5.2
PLnO	32.8	12.1	11.1	11.7	7.2	5.5	6.3	1.6	1.8
OOO	33.8	9.1	13.6	14.9	11.8	6.1	3.1	1.3	1.0
PLO	37.1	11.3	13.7	13.0	9.0	3.9	1.8	0.6	0.1
ELnO	38.7	1.9	2.1	2.6	2.5	—	--	—	—
OLnO	38.9	2.1	1.2	1.2	1.1	—	—	—	—
OLO	39.1	3.8	2.0	1.8	1.3	—	—	—	—
PLL	39.3	4.0	4.1	2.6	0.3	—	—	—	—
LLO	42.6	14.9	11.0	5.5	1.8	—	—	—	—
LLL	48.1	6.7	2.6	0.7	0.1	—	—	—	—

[a]Retention times in silver–high-performance liquid chromatography (Ag-HPLC).
[b]Abbreviations: S, stearic acid; P, palmitic acid; O, oleic acid; L, linoleic acid; Ln, linoelaidic acid; E, elaidic acid.

TABLE 5
TAG Composition of Samples Taken During the Second Hydrogenation

		Sample							
TAG	t_R[a] (min)	9	10	11	12	13	14	15	16
SEE[b]	7.6	—	—	—	—	—	3.1	1.9	3.7
OPE	14.7	—	—	—	—	6.6	5.5	7.1	5.9
OSE	15.5	—	—	—	2.6	3.9	13.5	17.7	21.7
EEE	17.5	—	2.4	1.4	4.7	5.4	8.0	12.3	11.4
POO	17.9	—	0.7	0.8	1.0	2.3	2.2	4.3	2.8
SOO	18.4	—	1.2	1.0	1.8	2.2	2.2	2.5	2.9
OPO	20.4	—	3.6	3.2	6.5	11.0	10.5	12.3	22.5
EEO	26.2	5.7	10.9	16.6	24.3	31.9	28.3	22.1	14.4
SLnS	30.9	6.1	8.0	12.8	13.4	14.3	14.1	9.4	4.4
EOO	31.2	1.6	5.3	4.6	4.6	3.4	1.9	0.6	—
PLnO	32.8	2.1	6.2	3.5	2.5	3.5	1.1	—	—
OOO	33.8	14.9	16.3	11.1	7.4	3.5	1.1	—	—
SLnO	34.8	13.4	11.8	13.8	9.1	2.9	0.5	—	—
PLO	37.1	15.9	12.1	10.0	7.5	1.9	0.3	—	—
ELnO	38.7	2.0	1.4	1.0	0.6	—	—	—	—
OLO	39.1	3.2	1.4	0.7	0.2	—	—	—	—
PLL	39.3	4.6	3.0	1.4	0.6	—	—	—	—
LLO	42./6	16.8	9.1	4.5	1.3	—	—	—	—
LLL	48.1	5.2	2.0	0.1	—	—	—	—	—

[a]Retention times in Ag-HPLC.
[b]See Table 4 for abbreviations.

samples 13–16 (Table 5) did not possess these TAG, which is in agreement with the decrease of L shown in Table 3. PLO and OOO percentages started to increase after 45 min of hydrogenation; after 90 min, they started to diminish to values around 1.0% or less (first hydrogenation). For the second hydrogenation PLO and OOO levels initially increased, and then diminished to nondetectable levels (samples 15 and 16). During both hydrogenation processes, TAG with more saturated and *trans* fatty acids were formed. Only the main TAG were included in Tables 4 and 5. At the beginning of hydrogenation, TAG with long retention times diminished while intermediate retention-time TAG were formed. They are presented in high percentages in samples 1–4 (Table 4) and samples 9–12 (Table 5). Then after 90 min of the start of the reaction, intermediate retention-time TAG diminished as short retention-time ones increased. The TAG compositions of samples 6–8 and 14–16 were different as expected. OSE, EEE, and EEO values, especially, were different. OSE and EEE were present in much higher percentages in samples 14–16 compared to the percentages found for samples 6–8. EEO was the main TAG in samples 6–8. Sample 14 has higher percentages of OSE and EEE than sample 8, but lower than samples 15 and 16 and the highest percentage of EEO of the three last samples taken during the second hydrogenation process (14, 15, and 16).

Even though fatty acid composition was similar, TAG structure was different. The differences in TAG structure were responsible for the differences observed in the crystallization behavior.

Induction times of crystallization. The results of analysis of 16 samples by the two methods (microscopy and laser polarized turbidimetry) are shown in Table 6, with the temperatures selected in each case. Temperatures were selected taking into account their MDP since when a very low temperature is selected there is no induction period and therefore the sample crystallizes before the cell can reach crystallization temperature. The induction times varied from about 10 to 60 min. Every sample was measured seven times by the laser and seven times by microscopy. Means and standard deviations

TABLE 6
Comparison of Obtained Values for Induction Times of 16 Different Samples Determined by Microscopy and a Laser Polarized Light Turbidimetry

Sample	Crystallization temperature (K)	Laser optical setup ($n = 7$)	Microscopy ($n = 7$)
1	290.2	60.0 ± 1.7	65.3 ± 3.5[a,b]
2	289.9	17.3 ± 1.0	22.2 ± 1.6[a,b]
3	293.8	31.6 ± 1.0	33.6 ± 1.8[a]
4	295.1	20.7 ± 0.8	25.2 ± 2.3[a,b]
5	295.4	10.9 ± 0.5	15.7 ± 1.1[a,b]
6	298.3	12.1 ± 0.5	17.6 ± 1.5[a,b]
7	300.4	14.6 ± 0.6	15.3 ± 0.8
8	303.2	23.3 ± 0.9	29.8 ± 1.9[a,b]
9	290.6	46.7 ± 0.9	50.1 ± 2.9[a]
10	291.6	32.7 ± 1.2	35.6 ± 2.3[a]
11	293.3	32.6 ± 0.9	34.8 ± 2.0[a]
12	295.6	26.9 ± 0.8	29.0 ± 1.5[a]
13	296.3	9.8 ± 0.3	12.2 ± 0.8[a,b]
14	302.1	16.4 ± 0.5	20.1 ± 1.2[a,b]
15	305.7	14.1 ± 0.7	17.0 ± 1.5[a,b]
16	307.1	11.4 ± 0.4	13.2 ± 1.0[a,b]

[a]Value (mean of the indicated sample ± SD) for the samples bearing a superscript letter are significantly different ($P < 0.05$, paired Student's *t*-test) with respect to the optical setup value.
[b]$P < 0.01$. *n*, number of analysis.

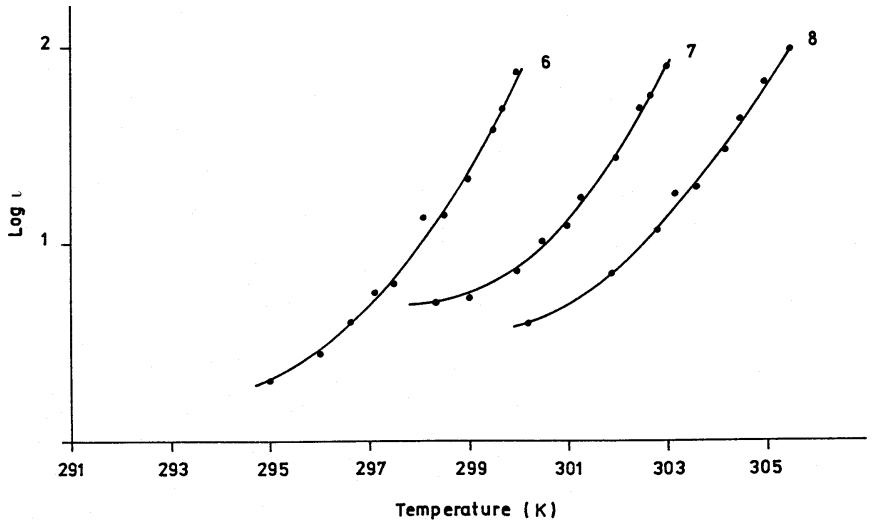

FIG. 2. Log ι (induction times of crystallization) vs. temperature for samples 6, 7, and 8.

are shown in Table 6. For every sample, the same crystallization temperature and supercooling and cooling rates were used for both methods. This procedure was repeated for 16 samples.

Standard deviations were higher when induction times were measured by microscopy. Also, significant differences were found between means at $P < 0.05$ for paired Student's *t*-test and at $P < 0.01$. The microscopy method has been used for a long time. The time of appearance measured by microscopy is not equivalent to the time of nucleation measured by the laser optical setup, since the crystals must reach a minimum size of 0.2 μm to be detected with a microscope and the laser can see nuclei of smaller size. Crystals can be seen for these two methods because they are birefringent and therefore they reflect the light at two different rates, giving a circular beam and an elliptic one. As a light coming from a laser has a narrow band and is polarized, and the resulting beam has all the wave components in the same orientation, these add to each other and make this equipment very sensitive. Nuclei of smaller size can be detected and therefore the measured induction times are shorter. When natural light is used as a light source instead of a laser, wave components cancel between each other and there is a loss of sensitivity. The results which can be obtained are very dependent on the light source. In addition, the microscope method has the disadvantage of being dependent on the operator. The laser method is more objective and a less trained operator can obtain more accurate data.

Nucleation study. Induction times (ι) at different t_c were measured with the laser optical setup for samples 6–8 and 14–16. Curves of log ι vs. temperature are plotted in Figures 2 and 3. There were no induction times under 293, 295, and 297 K for samples 6, 7, and 8, and under 297, 303, and 304 K for samples 14, 15, and 16, respectively. These values are in agreement with their MDP within the same hydrogenation process. The higher the MDP, the higher the temperature

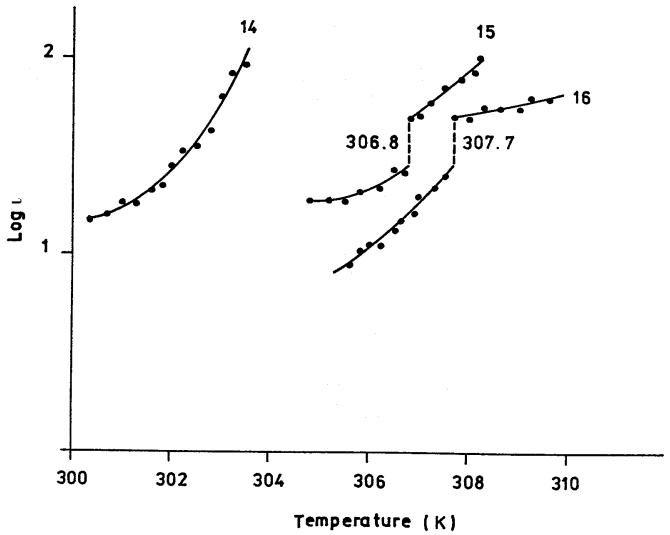

FIG. 3. Log ι (induction times of crystallization) vs. temperature for samples 14, 15, and 16.

under which there was no induction time. Sample 14 should have had induction times much closer to the ones obtained for sample 7. However, the times were intermediate between the times found for samples 7 and 8. Nucleation behavior was different between the two hydrogenation processes because even if the MDP were similar, the TAG composition of the samples was different. According to the chemical composition, two different behaviors were found. For samples 6–8 and 14, a continuous curve can be drawn, while for samples 15 and 16 there was a discontinuity in the nucleation curve at 306.8 and 307.7 K, respectively. This means that when samples 6–8 and 14 were crystallized from the melt, just one polymorphic form was obtained and was the same for every temperature. On the contrary, the discontinuity of samples 15 and 16 curves clearly demarcated the occurrence of one polymorph from another, as samples nucleated below a given temperature in β′ form and above it in β form. To confirm this hypothesis, crystals were analyzed for their polymorphic form by powder XRD. The diffraction patterns of samples 6–8 and 14 showed two strong signals at 3.9 and 4.3 Å. These samples were found to nucleate in the β′ form even at the highest measured temperatures, which are very close to the melting points. The first parts of curves 15 and 16 also presented a β′ pattern. However, the second parts of them corresponded to the nucleation of the β form. A characteristic pattern of the β form with a strong signal at 4.6 Å was obtained by powder XRD for both samples.

From the results reported for OSE, EEE, and EEO in Tables 4 and 5, it can be noticed that the percentage of OSE and EEE always increased with time but in amounts very different for both processes. EEO always increased during the first hydrogenation while during the second hydrogenation, EEO initially increased, reached the highest value (sample 13), and then decreased to a value markedly lower (sample 16) than the one of sample 8. Samples 15 and 16 have a higher EEE and OSE content than the others and have a lower content of EEO. No reports of a stable β′ form of EEE were found in the literature. When EEE is mixed with other TAG, such as PPP, the β′ form is destabilized (19). The crystallization behavior of samples 15 and 16 is more polymorphic, similar to the behavior of semisolid natural fats such as palm oil. The polymorphic form in which these samples crystallized depended on crystallization temperature, and both β′ and β could be obtained from the melt. Samples with lower EEE content crystallized in the β′ form, and no β form was obtained from the melt even at crystallization temperatures very close to the melting point. The crystallization behavior was closely related to the TAG present in the oil, and especially to E-containing TAG.

Activation free energy of nucleation. The activation free energies of these samples, which were calculated from the Fisher-Turnbull equation, are reported in Tables 7 and 8 as well as the crystallization temperatures and the supercoolings $\Delta T = (T_m - T_c)$. MDP for samples 6–8 and 14–16 were reported in Table 1 and the slopes were 0.048 10^5, 0.017 10^5, 0.006 10^5, 0.111 10^5, 0.093 10^5, and 0.115 10^5, respectively, for the β′ forms, and 0.033 10^5 and 0.008 10^5 for the β forms of samples 15 and 16.

For the same degree of supercooling, the β′ form of sample 14 had greater activation free energy of nucleation than samples 6–8. Sample 8 had the lowest values of ΔG_c. Nucleation of the β′ crystal was fastest in sample 8 and slowest in sample 14. Samples 15 and 16 crystallized in the β form above 306.7 and 307.6 K, respectively. At these high temperatures, ΔG_c was very low for the β form and therefore the nucleation in this form was preferred. From induction times of crystallization, ΔG_c can be calculated and from these values the possibility of occurrence of a polymorphic form can be understood. The crystallization behavior was found to be closely related to TAG content of E. Samples 15 and 16, with a high content of EEE, had a low activation free energy for β form at crystallization temperatures close to the melting point, while samples with low EEE content and a higher mixed elaidic acid TAG content did not show the β form. In samples 15 and 16, EEE led crystallization under β form at temperatures close to the melting point.

Induction time values of hydrogenated sunflower oil indicate that nucleation in sunflower oil is very fast and ΔG_c indi-

TABLE 7
Activation Free Energy of Nucleation for Different Temperatures at Different Supercoolings: First Hydrogenation

Sample 6			Sample 7			Sample 8		
Temp.[a] (K)	ΔG_c (Kj/mol)	ΔT^2 (K)	Temp. (K)	ΔG_c (Kj/mol)	ΔT^2 (K)	Temp.[a] (K)	ΔG_c (Kj/mol)	ΔT^2 (K)
295.0	0.6	64	298.3	0.3	47.6	300.2	0.1	43.6
296.0	0.8	49	299.0	0.3	40.9	301.9	0.2	24.0
296.6	1.0	40.9	300.0	0.5	27.0	302.8	0.3	16
297.1	1.1	34.8	300.5	0.6	24.0	303.2	0.4	12.9
297.5	1.3	30.2	301.0	0.7	19.4	303.6	0.5	10.2
298.1	1.7	24.0	301.3	0.8	16.8	304.2	0.7	6.7
298.5	2.0	20.2	302.0	1.2	11.6	304.5	0.9	5.3
299.0	2.5	16	302.7	1.9	7.3	305.0	1.5	3.2
299.5	3.3	12.2	303.2	2.9	4.8	305.5	2.9	1.7
299.7	3.7	10.9						
300.0	4.4	9						

[a]Temp., temperature.

TABLE 8
Activation Free Energy of Nucleation for Different Temperatures at Different Supercoolings: Second Hydrogenation

Sample 14			Sample 15			Sample 16		
Temp.[a] (K)	ΔG_c (Kj/mol)	ΔT^2 (K)	Temp. (K)	ΔG_c (Kj/mol)	ΔT^2 (K)	Temp.[a] (K)	ΔG_c (Kj/mol)	ΔT^2 (K)
300.4	3.7	25	304.8	3.1	25	305.6	1.6	60.8
300.7	4.2	22.1	305.2	3.6	21.2	305.8	1.6	57.8
301.0	4.8	19.4	305.5	4.2	18.5	306.0	1.7	54.8
301.3	5.5	16.8	305.8	4.8	16	306.2	1.8	51.8
301.6	6.4	14.4	306.2	5.9	13.0	306.5	2.0	47.6
301.8	7.1	13.0	306.5	7.1	10.9	306.6	2.1	46.2
302.0	8.0	11.6	306.7	8.0	9.6	306.9	2.2	42.2
302.2	9.0	10.2	306.8	3.0	9	307.0	2.3	41.0
302.5	11.0	8.4	307.0	3.5	7.8	307.3	2.5	37.2
302.8	13.6	6.8	307.2	4.1	6.7	307.5	2.7	34.8
303.0	16.0	5.8	307.5	5.2	5.2	307.7	0.2	32.5
303.2	19.1	4.8	307.8	6.9	4	308.0	0.2	29.2
303.5	25.5	3.6	308.1	9.5	9.4	308.3	0.2	26.0
			308.2	10.7	10.7	308.6	0.3	23.0
						309.0	0.3	19.4
						309.2	0.4	17.6
						309.6	0.5	14.4

[a]Temp., temperature.

cate a very low supercooling is needed, since even at crystallization temperatures close to the MDP, crystallization occurred at shorter times than the ones reported for other fats (13). These results are also very important from the practical point of view for processing design, especially in regard to the processes in which fats should be completely crystallized by the end of the production line.

ACKNOWLEDGMENTS

We are grateful to W. Atencio and A. Campana for expert technical assistance. This work was supported by funds from SECYT (Secretaría de Ciencia y Tecnología) (Prog. Bid 802 OC-AR/ Pid 0357), Argentina.

REFERENCES

1. Haumann, B.F., Tools Hydrogenation, Interesterification, *INFORM 5*:668–678 (1994).
2. Rodrigo, M.T., and S. Mendioroz, A New Catalyst for the Selective Hydrogenation of Sunflower Seed Oil, *J. Am. Oil Chem. Soc. 69*:802–805 (1992).
3. Allen, R.R., Hydrogenation, *Ibid. 58*:166–169 (1981).
4. Lawson, H., Physical Properties, in *Food Oils and Fats,* edited by H. Lawson, Chapman & Hall, New York, 1995, p. 29.
5. Hartel, R.W., Applications of Milk-Fat Fractions in Confectionary Products, *J. Am. Oil Chem. Soc. 73*:945–953 (1996).
6. Larsson, K., Lipids in the Solid State, in *Lipids—Molecular Organization, Physical Functions and Technical Applications,* edited by K. Larsson, The Oily Press, Glasgow, 1994, p. 38.
7. Brimberg, U., The Kinetics of Melting Crystallization of Cocoa Butter, *Fette Seifen Anstrichm. 87*:295–301 (1985).
8. Hachiya, I., T. Koyano, and K. Sato, Seeding Effects on Solidification Behavior of Cocoa Butter and Dark Chocolate. I—Kinetics of Solidification, *J. Am. Oil Chem. Soc. 66*:1757–1762 (1989).
9. Hachiya, I., T. Koyano, and K. Sato, Seeding Effects on Crystallization Behavior of Cocoa Butter, *Agric. Biol. Chem. 53*:327–332 (1989).
10. Hausmann, A., H.D. Tscheuschner, and I. Tralles, Influence of Cooling Conditions on Crystallization of Chocolate, *Zucker Süsswaren Wirtsch. 46*:492–498 (1993).
11. Chaiseri, S., and P.S. Dimick, Dynamic Crystallization of Cocoa Butter. I—Characterization of Simple Lipids in Rapid- and Slow-Nucleating Cocoa Butters and Their Seed Crystals, *J. Am. Oil Chem. Soc. 72*:1491–1496 (1995).
12. Chaiseri, S., and P.S. Dimick, Dynamic Crystallization of Cocoa Butter. II—Morphological, Thermal, and Chemical Characteristics During Crystal Growth, *Ibid. 72*:1497–1504 (1995).
13. Ng, W.L., A Study of the Kinetics of Nucleation in a Palm Oil Melt, *Ibid. 67*:879–882 (1990).
14. Ng, W.L., and C.H. Oh, A Kinetic Study on Isothermal Crystallization of Palm Oil by Solid Fat Content Measurements, *Ibid. 71*:1135–1139 (1994).
15. van Putte, K.P.A.M., and B.H. Bakker, Crystallization Kinetics of Palm Oil, *Ibid. 64*:1138–1143 (1987).
16. Grall, D.S., and R.W. Hartel, Kinetics of Butterfat Crystallization, *Ibid. 69*:741–747 (1992).
17. Smith, K.W., J.M. Perkins, B.S.J. Jeffrey, and D.L. Phillips, Separation of Molecular Species of *cis*- and *trans*-Triacylglycerols in *trans*-Hardened Confectionery Fats by Silver-Ion High-Performance Liquid Chromatography, *Ibid. 71*:1219–1222 (1994).
18. Herrera, M.L., Crystallization Behavior of Hydrogenated Sunflowerseed Oil: Kinetics and Polymorphism, *Ibid. 71*: 1255–1260 (1994).
19. Desmedt, A., Etude des Propriétés Structurales et Thermiques de Triglycérides Purs et en Présence d'Emulsifiants. Influence de la Nature de la Chaîne en C 18 et Application au Phénomène de Blanchiment, Ph.D. Thesis, Facultés Universitaires, Notre-Dame de la Paix, Namur, 1993.

[Received September 5, 1997; accepted June 9, 1998]